

# Molecular Orientation of Extruded PET/LCP Blend Films. Part I: Polarized Infrared Spectroscopy

Marcia C. Branciforti, Lucineide B. Silva, Rosario E. S. Bretas

Department of Materials Engineering, Federal University of São Carlos, Rod. Washington Luis, Km 235, CEP13565-905, São Carlos, SP, Brazil

Received 6 December 2005; accepted 26 February 2006

DOI 10.1002/app.24395

Published online in Wiley InterScience (www.interscience.wiley.com).

**ABSTRACT:** The polarized infrared (IR) spectroscopy technique was used to evaluate the surface uniaxial molecular orientation of films of poly(ethylene terephthalate) (PET), two thermotropic liquid crystalline polymers (LCPs), Vectra<sup>®</sup>A950 and Rodrun<sup>®</sup>LC5000, and their blends obtained by extrusion. The molecular orientation of the LCP and of the crystalline and amorphous PET phases in the draw direction was evaluated along the transverse section of the films and as a function of the blend composition. A compatibilizer agent was used to improve the interfacial adhesion between the PET and LCPs. The results showed that the surface molecular orientation of both LCPs was very high along the draw direction. However, when blended, the orientation of the LCP phase decreased drastically, it was dependent of its content and varied along the

transverse section of the extruded films. The maximum orientation was observed in the blend with 5 wt % LCP content and at the position where the shear rate was maxima. The LCP Vectra<sup>®</sup>A950 showed higher orientation than the Rodrun<sup>®</sup>LC5000, as a pure material and as blended. For the PET phases, an alignment of the amorphous phase in the draw direction due to the presence of LCP and compatibilizer agent was observed. The crystalline phase of PET, however, showed no significant orientation in the draw direction. The compatibilizer agent proved efficient for both PET/LCP systems. © 2006 Wiley Periodicals, Inc. *J Appl Polym Sci* 102: 2241–2248, 2006

**Key words:** molecular orientation; dichroism; liquid crystalline polymer; poly(ethylene terephthalate)

## INTRODUCTION

Several investigators<sup>1–17</sup> have attempted to achieve composite-like materials by reinforcing a thermoplastic with a thermotropic liquid crystalline polymer (LCP). Most of the physical and mechanical properties of these composites and their processability behavior are partially or totally dependent on the degree of the molecular orientation, which results of the melt processing and relaxation effects. It has been demonstrated that the molecular orientation in the draw direction of these blends increases with the LCP content, due to the uniaxial orientation of the LCP. The major contribution to the tensile modulus of these blends comes from the molecular orientation of the LCP phase, which increases as the draw ratio increases. Reinforcing effects have been observed in PET/Vectra blends processed at conditions of high extensional flow such extrusion or spinning with high draw ratios.<sup>3,17–22</sup> The application of a specific compatibilizer can improve the adhesion between the phases and consequently enhance the mechanical properties.

The molecular orientation of LCPs has been characterized by Bensaad and coworkers<sup>23,24</sup> and by Kaito and coworkers,<sup>25–28</sup> using infrared (IR) spectroscopy. It was demonstrated that the orientation is determined by the flow history of the polymer melt and by the cooling conditions. In extrudates of LCPs, the surface orientation is equivalent to the bulk orientation at drawdown ratios above 4.0. The surface orientation tends to be higher than the bulk orientation at lower drawdown ratio. In injection-molded LCPs, it was observed that the orientation is maximum along the principal axis of the mold with two significant minima of orientation located near the injection gate. Furthermore, along the transverse direction toward the mold edge, there is a marked fall-off in orientation, being the orientation minima at positions near the gate. It was also observed that there was an ideal melting temperature at which the maximum orientation was obtained.

The molecular orientation can be determined by various techniques; for example, wide-angle X-ray diffraction (WAXD), birefringence, polarized Fourier transform infrared spectroscopy (FTIR), specular reflection spectroscopy, and <sup>13</sup>C and <sup>1</sup>H nuclear magnetic resonance (NMR). Polarized FTIR is one of the most convenient methods that can be used to quantify directly the degree of molecular orientation in crystalline and amorphous regions in polymer films.<sup>29–32</sup>

Correspondence to: R. E. S. Bretas (bretas@power.ufscar.br).

Contract grant sponsor: Fundação de Amparo a Pesquisa do Estado de São Paulo (FAPESP).

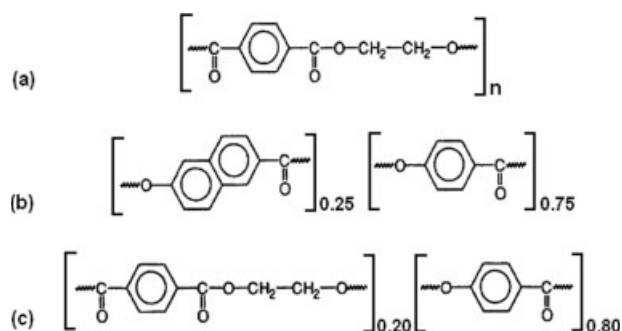


**Figure 1** Chemical structures of (a) PET, (b) Vectra<sup>®</sup>A950, and (c) Rodrun<sup>®</sup>LC5000.

In the present work, we report the molecular orientation of both components in blends of poly(ethylene terephthalate) (PET) and two thermotropic LCPs, these last ones differing in molecular structure. The orientation was determined by polarized IR spectroscopy and analyzed as a function of blend composition and along the transverse section of the extruded films. Both LCPs and the PET have characteristic absorption bands in their IR spectrum, allowing the measurement of the individual molecular orientation of both polymers and consequently, the crystalline and amorphous phase orientation in the blends. The effect of a compatibilizer agent was also evaluated. In this work we will restrict our attention to the molecular orientation development in the skin layer. The bulk molecular orientation study by wide angle X-ray diffraction pole figures will be the focus of another paper.<sup>33</sup>

## EXPERIMENTAL

### Materials

The PET resin used was a copolymer based on terephthalic acid and ethylene glycol, kindly donated by Rhodia Ster of Brazil, known as RhoPET S80. The PET weight average (MW) was 30,000 g/mol and its melting temperature ( $T_m$ ) was 235°C. Two thermotropic LCPs were used to make blends with the PET resin. One LCP was a random copolyester of 75 mol % of poly(hydroxybenzoic acid) (HBA) and 25 mol % of poly(hydroxynaphthoic acid) (HNA), Vectra<sup>®</sup>A950, supplied by Ticona (Florence, KY, USA), and its MW and  $T_m$  were 30,000 g/mol and 280°C, respectively. The other LCP was formed by 80 mol% HBA and 20 mol% poly(ethylene terephthalate), Rodrun<sup>®</sup>LC5000, supplied by Unitika Co., Ltd. (Tokyo, Japan). The MW and  $T_m$  were 20,000 g/mol and 280°C, respectively. The compatibilizer agent Lotader<sup>®</sup>AX8900 was used to enhance the interfacial adhesion between the PET and the LCPs. This compatibilizer was supplied by Atofina of France and is a random terpolymer of 67 wt% of ethylene, 25 wt% of acrylic ester and 8 wt% of glycidyl methacrylate, and its  $T_m$  was 60°C. Their

chemical compositions are shown in Figure 1. These materials were dried in a vacuum oven at 150°C for 5 h before blending.

### Blending and film extrusion

First, a master batch of 80/20 LCP/compatibilizing agent was made by twin screw extrusion in a co-rotational ZSK30 Werner and Pfleiderer extruder, at a flow rate of 10 kg/h, 100 rpm, and die temperature of 270–275°C.

The films of the blends were subsequently produced in the same twin screw extruder, using a slit die and a set of rollers, as shown in Figure 2. The extruder flow rate was between 2 and 4 kg/h, the screws rotation was varied between 80 and 100 rpm, and the die temperature was set at 240°C, depending on the blend composition. The slit die was a T-type die, with 45° convergence angle, width of 100 mm, and a gap between the lips of 0.4 mm. The ratio between the die width and the film width was varied between 1 and 1.7. The average drawdown rate was 6 m/min. Films with compositions PET/LCP 100/0, 95/5, 90/10, 85/15, and 0/100 and PET/LCP/compatibilizing agent 90/10/2.5, in wt % were thus produced.<sup>34</sup>

### Polarized infrared spectroscopy

The molecular orientation of the LCP and PET phases of the extruded films was analyzed by polarized IR spectroscopy. A FTIR spectrometer model Spectrum 1000, equipped with a AgBr wire grid polarizer and with a variable angle specular reflectance accessory (both from Perkin-Elmer), were used to record the reflection spectra with the polarized direction parallel and perpendicular to the draw direction, without altering the sample position. All the IR spectra were obtained at an incident angle of 45° and at room temperature. The extrusion direction was set perpendicular to the plane of incidence. Each spectrum was an average of 128 scans at the resolution of 4 cm<sup>-1</sup>. The measured reflectance for each polarization was corrected by the Kramers–Kronig transformation before analysis.

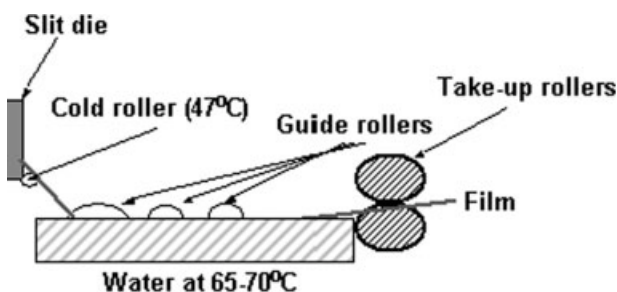


**Figure 2** Schematic representation of the films processing.

The orientation measurements were performed at four different and equidistant positions located along the films width (from the center to the wall), as shown in Figure 3. The spot size of the IR radiation was adjusted using a mask with a 5-mm diameter opening. The abbreviations *c*, *nc*, *nw*, and *w* represent center, near the center, near the wall, and at the wall of the film (0.5 mm from the film edge), respectively. Five measurements were made at each position and on every blend sample to obtain significant statistical average of the data.

The absorption intensities were obtained by integrating the area under the absorption bands. The dichroic ratio (*DR*) of the analyzed bands was calculated from the ratio of the absorption intensities measured with the IR radiation polarized parallel to ( $A_{\parallel}$ ) and perpendicular to ( $A_{\perp}$ ) the draw direction, as given by the following equation:

$$DR = \frac{A_{\parallel}}{A_{\perp}} \quad (1)$$

For a uniaxially drawn material, the molecular orientation is sufficiently described by the Hermans orientation factor. The orientation is defined as a function of the distribution factor of the angle between the polymer chain axis and the draw direction. If uniaxial orientation is assumed, the Hermans orientation factor of the transition moment of the particular absorption band ( $f_i$ ) can be calculated by

$$f_i = \frac{(DR - 1)}{(DR + 2)} \quad (2)$$

If the angle between the transition moment vectors and the chain axis ( $\alpha$ ) is known, the Hermans orientation factor of the molecular chain axis ( $f$ ) can be calculated by

$$f = \frac{2f_i}{(\cos^2 \alpha - 1)} \quad (3)$$

In this work, the absorption bands at 1474 and 1630  $\text{cm}^{-1}$  were used to characterize the chain orienta-

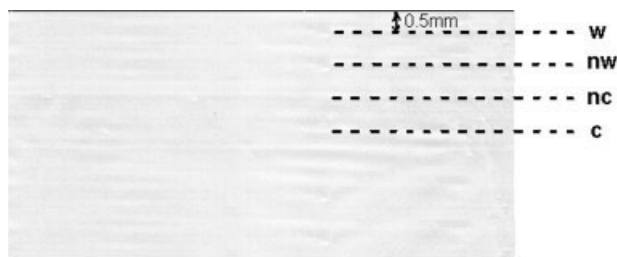


**Figure 3** The four positions along the transverse section of the blend extruded films where the molecular orientation was analyzed, where (*w*) at the wall; (*nw*) near the wall; (*nc*) near the center and (*c*) center position.

tion of the Vectra<sup>®</sup>A950 LCP phase. These bands are assigned to the ( $-\text{C}=\text{C}-$ ) stretching vibration of the naphthalene (monomer HNA) and benzene (monomer HBA) rings, respectively.<sup>25,35</sup> The band at 1601  $\text{cm}^{-1}$ , assigned to the stretching mode of ( $-\text{C}=\text{C}-$ ) in the benzene ring, was used to characterize the chain orientation of the Rodrun<sup>®</sup>LC5000 LCP phase.<sup>11</sup> It is well known that the PET IR spectrum exhibits numerous absorption bands with dichroic nature. However, in this study, because of the similarity between the IR spectra of the PET and the LCPs, two pair of bands, at 974 and 1453  $\text{cm}^{-1}$  and 1340 and 1370  $\text{cm}^{-1}$ , which did not overlap with any absorption bands of the LCPs, were used to determine the degree of molecular orientation of the amorphous and crystalline PET phases. The absorption band at 974  $\text{cm}^{-1}$  is associated with the  $\text{CH}_2$  vibration mode of the *trans* conformers. The band at 1340  $\text{cm}^{-1}$  is attributed to the  $\text{CH}_2$  wagging mode of the glycol segments in the *trans* conformer. It is associated predominantly with crystalline domains, although *trans* segments can be present in amorphous domains of the polymer. The bands at 1370 and 1453  $\text{cm}^{-1}$  are assigned to the  $\text{CH}_2$  wagging and bending mode, respectively, of the glycol segments in the *gauche* conformer.<sup>27</sup> The *gauche* conformer can only exist within the amorphous domains of the polymer. The angle  $\alpha$  is 22° for the 1474- $\text{cm}^{-1}$  band,<sup>35,36</sup> 34° for the 974- $\text{cm}^{-1}$  band,<sup>27,37</sup> and 21° for the 1340- $\text{cm}^{-1}$  band.<sup>27,29,31,38,39</sup> The value of  $\alpha$  is unknown for the 1630, 1601, 1453, and 1370- $\text{cm}^{-1}$  bands. To overcome variations in the overall intensity of the spectra, arising from effects like surface quality and thickness variation of the samples, all spectra were normalized by examining the 794 and 1410- $\text{cm}^{-1}$  bands, which are insensitive to orientation as well as crystallinity. These bands are assigned to benzene ring vibration of the PET.<sup>31,40,41</sup> A single spectrum was defined as the reference spectrum, and the areas of these peaks in this spectrum were measured. All other spectra were then multiplied by a factor that made the areas of their 794 and 1410- $\text{cm}^{-1}$  peaks equal to that of the reference spectrum.

## RESULTS AND DISCUSSION

Typical IR spectra of both LCPs films, Vectra<sup>®</sup>A950, and Rodrun<sup>®</sup>LC5000, with polarization directions parallel (full line) and perpendicular (dashed line) to the draw direction, are shown in Figure 4(a) and (b), respectively. These spectra are measured at the position near the films center, *c*. The absorbance associated with the 1630- and 1474- $\text{cm}^{-1}$  bands for the Vectra<sup>®</sup>A950 LCP and 1601- $\text{cm}^{-1}$  band for the Rodrun<sup>®</sup>LC5000 is stronger along the director (draw direction). This is an indication that the transition moment vectors direction of the corresponding

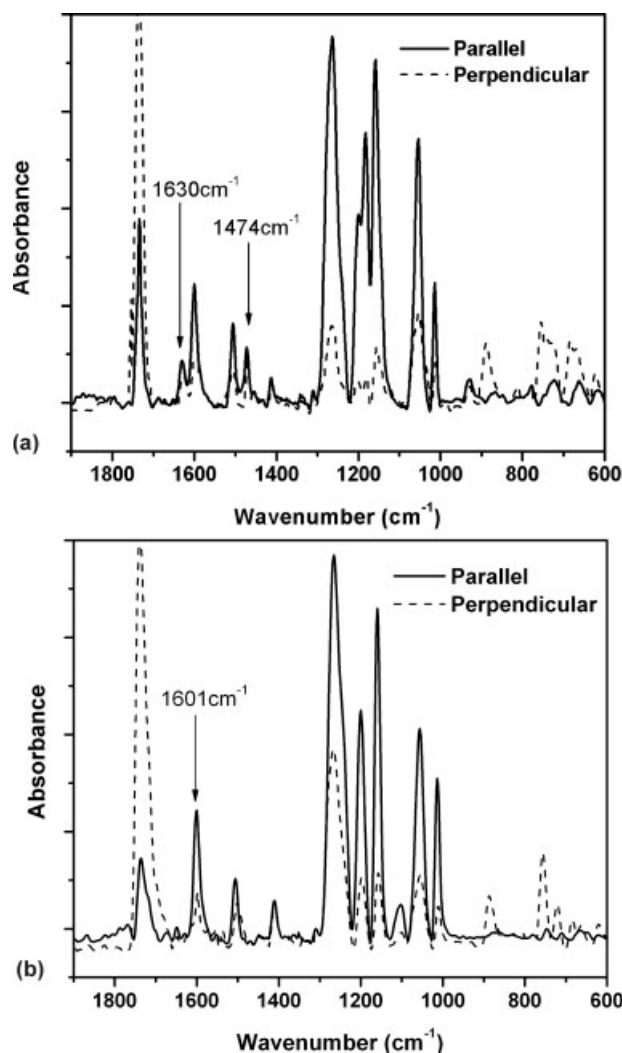


**Figure 4** Infrared spectra of (a) Vectra<sup>®</sup>A950 and (b) Rodrun<sup>®</sup>LC5000 LCP using polarized light parallel and perpendicular to the draw direction and measured at the position near the film center.

vibrations should be essentially parallel to the long axis of both LCPs molecules, in agreement with previous reports.<sup>25,35,36</sup>

Examples of the parallel and perpendicular FTIR absorption spectra for the extruded PET/LCP films are illustrated in Figure 5. The spectra were recorded for the 95/5 PET/LCP Vectra<sup>®</sup>A950 film, Figure 5(a), and 85/15 PET/LCP Rodrun<sup>®</sup>LC5000 film, Figure 5(b), at the position near the films center, nc. Figure 5 shows the absorbance bands associated with both LCPs, the bands associated with the amorphous (G) and crystalline (T) PET phases, and the normalization (Norm.) bands at 794 and 1410  $\text{cm}^{-1}$ . The PET phase bands at 974, 1453, 1340, and 1370  $\text{cm}^{-1}$  are strongly dichroic and showed parallel character. These bands do not absorb strongly, avoiding saturation and are suitable for characterizing the molecular orientation of the PET phases in the PET/LCP blends.

### Molecular orientation of the LCP phase

The molecular orientation of the LCP phase in the PET/LCP films was characterized by the Hermans orientation factor ( $f$ ) from the characteristics absorption bands. Figures 6 and 7 show the calculated  $f$  based on equations (1), (2) and (3), for both PET/LCP Vectra<sup>®</sup>A950 and PET/LCP Rodrun<sup>®</sup>LC5000 blends, respectively. Typical standard deviation in  $f$  values is of the order of  $\pm 0.015$ . These figures show the variation of the LCP phase molecular orientation in the draw direction as a function of the blend composition and along the transverse section of the extruded films. It can be observed that the molecular orientation in the draw direction of the LCP phase, for both LCPs, decreased drastically in the PET/LCP blends. However, the decrease was lower for both 95/5 PET/LCP blends. The orientation factor of the LCP phase mark-

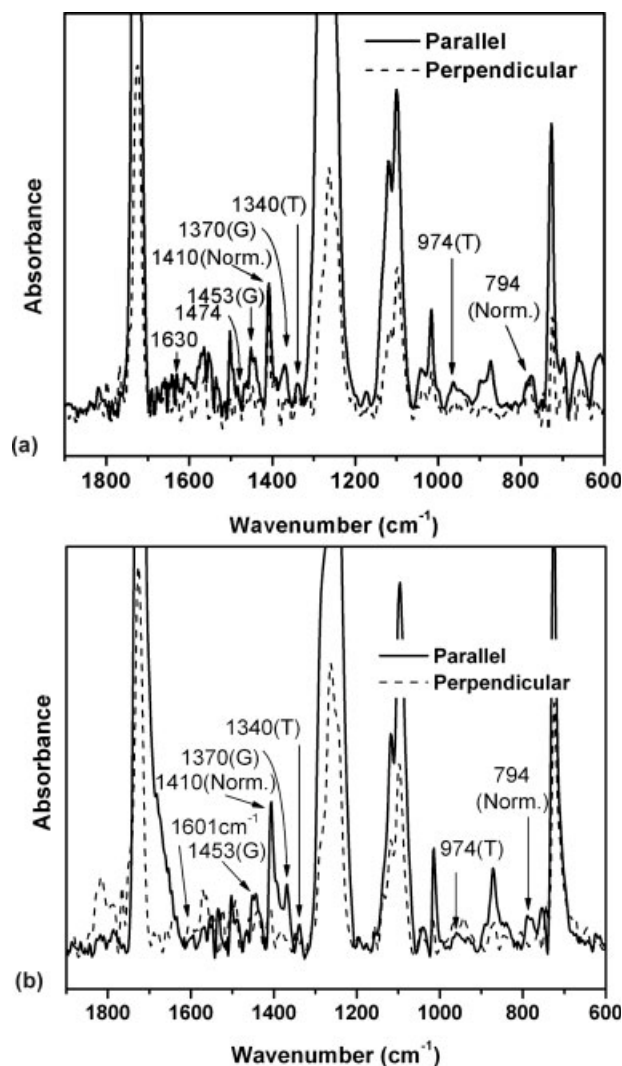


**Figure 5** Infrared spectra of (a) 95/5 PET/LCP Vectra<sup>®</sup>A950 and (b) 85/15 PET/LCP Rodrun<sup>®</sup>LC5000 blends using polarized light parallel and perpendicular to the draw direction and measured at the position near the films center.

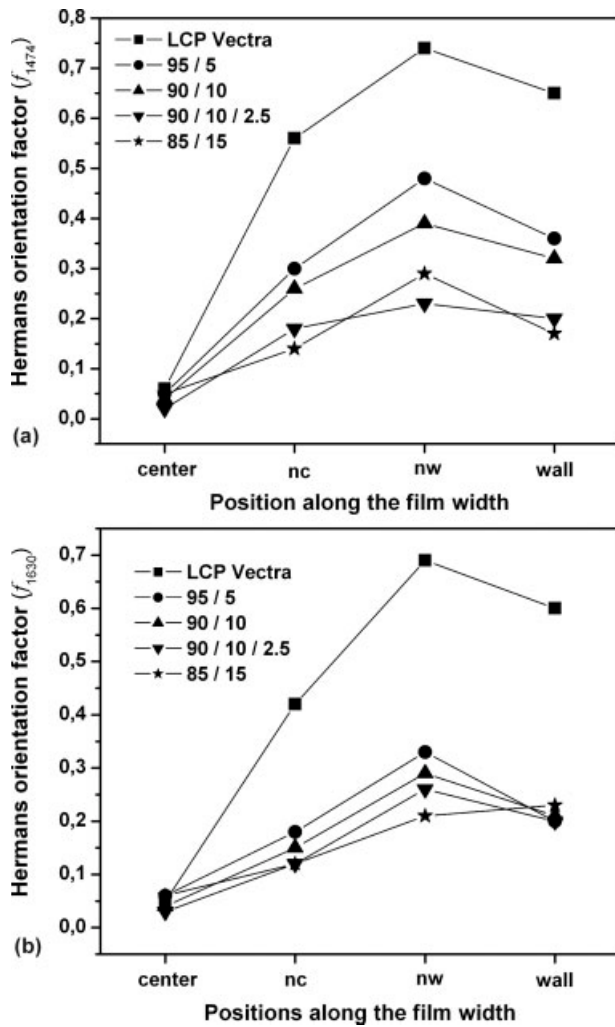


**Figure 6** Hermans orientation factor of the (a) 1474-cm<sup>-1</sup> band and (b) 1630-cm<sup>-1</sup> band for the PET/LCP Vectra® A950 blends along the transverse section of the extruded films.

edly decreased with the increase of the LCP content in both PET/LCP blends systems. In an earlier study,<sup>42</sup> it was observed that of all the blends, the 95/5 had the lowest elongational viscosity and it was the only one in which transesterification reactions occurred. Therefore, that blend was easier to draw than the others, allowing it to obtain a higher orientation. This behavior was attributed to a better dispersion of the LCP phase in this blend.

Concerning the variation of the LCP chain molecular orientation along the transverse section of the extruded films, also shown in Figures 6 and 7, it is observed that the orientation factor in the draw direction of the Vectra® A950 LCP phase increased as the distance from the center of the films increased. However at a distance of 0.5 mm from the film edge, the molecular orientation decreased again. In the film center the LCP phase orientation was almost zero. The maximum orientation of the LCP phase is observed at

the position immediately before the position near the wall. This behavior is similar to the shear rate behavior. In a slit die, the shear rate  $\dot{\gamma} = dv_x/dy$ , where  $v_x$  = velocity along the flow direction, of a power-law fluid is zero at the center (where the velocity profile is flat) and maximum near the wall (where the velocity decreases toward the wall).<sup>43</sup> Thus, the LCP orientational behavior is attributable to the shear rate effects.

Similar behavior is observed for the Rodrun® LC5000 LCP phase. Owing to its more rigid structure, the orientation degree of the Vectra® A950, as a pure film or in the PET/LCP blends, was higher than that of the Rodrun® LC5000 at the same processing conditions.

Lower values of  $f$  for the LCPs phases of the compatibilized blends were obtained relative to the 90/10 PET/LCPs blends. This is an indication that the compatibilizer agent reduced the molecular orientation of the LCP phase in the compatibilized blends. This result suggests an increased adhesion between the components of the blends and, as a consequence, a decrease in the molecular motion of both LCPs in the draw direction. A comparison of the  $f$  values reveals that the compatibilization was more effective between the PET and the Vectra® A950 LCP than the PET and the Rodrun® LC5000 LCP at the same processing conditions, as can be seen in Figures 6 and 7. It is known that the compatibilizer usually decreases the size of LCP domains. Morphological studies of the same films revealed that the compatibilized blend had a number of LCP fibrils per area higher than the uncompatibilized one, and these fibrils had smaller dimensions than in the noncompatibilized blend.<sup>42</sup> Paul and Bucknall<sup>44</sup> concluded that in blends of PET with LCPs, the compatibilizer can react with the PET or with the LCP. An effective

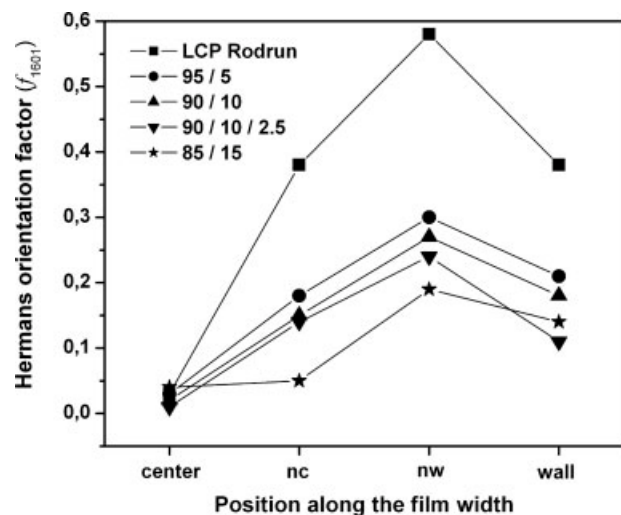


**Figure 7** Hermans orientation factor of the 1601-cm<sup>-1</sup> band for the PET/LCP Rodrun® LC5000 blends along the transverse section of the extruded films.

**TABLE I**  
Average Hermans Orientation Factors ( $f$ ) of the Crystalline (974 and 1340  $\text{cm}^{-1}$ ) and Amorphous (1453 and 1370  $\text{cm}^{-1}$ ) PET Phases of PET/LCP Blends as a Function of the Composition and along the Transverse Section of the Extruded

Blend PET/LCP	Pos. <sup>a</sup>	Vectra <sup>®</sup> A950				Rodrun <sup>®</sup> LC5000			
		$f_{974}$	$f_{1340}$	$f_{1453}$	$f_{1370}$	$f_{974}$	$f_{1340}$	$f_{1453}$	$f_{1370}$
100/0	c	0.20	0.21	0.02	0.02	0.20	0.21	0.02	0.02
	nc	0.25	0.26	0.04	0.03	0.25	0.26	0.04	0.03
	nw	0.26	0.28	0.06	0.05	0.26	0.28	0.06	0.05
	w	0.25	0.27	0.05	0.04	0.25	0.27	0.05	0.04
95/5	c	0.23	0.23	0.10	0.09	0.21	0.22	0.06	0.06
	nc	0.27	0.28	0.14	0.15	0.26	0.27	0.15	0.13
	nw	0.29	0.30	0.21	0.19	0.27	0.28	0.20	0.16
90/7.5/2.5	w	0.27	0.28	0.16	0.17	0.25	0.27	0.17	0.10
	c	0.21	0.22	0.08	0.08	0.19	0.17	0.05	0.04
	nc	0.24	0.25	0.12	0.12	0.24	0.25	0.12	0.10
90/10	nw	0.27	0.28	0.19	0.16	0.26	0.27	0.16	0.14
	w	0.26	0.27	0.15	0.13	0.25	0.26	0.14	0.09
	c	0.22	0.24	0.08	0.06	0.18	0.18	0.04	0.03
85/15	nc	0.26	0.26	0.11	0.11	0.23	0.24	0.11	0.07
	nw	0.27	0.28	0.18	0.13	0.26	0.25	0.15	0.11
	w	0.25	0.25	0.14	0.12	0.24	0.23	0.12	0.09
85/15	c	0.22	0.24	0.09	0.07	0.18	0.16	0.04	0.03
	nc	0.27	0.27	0.13	0.11	0.20	0.23	0.08	0.07
	nw	0.28	0.29	0.18	0.16	0.24	0.25	0.12	0.11
	w	0.26	0.28	0.15	0.12	0.21	0.19	0.08	0.09

<sup>a</sup> Positions along the transverse section of the extruded films: c, center position; nc, near the center; nw, near the wall; w, at the wall.

compatibilizer is located in the PET/LCP interphase, can decrease the interfacial tension, stabilize the morphology, and produce a narrower size distribution and a decrease in the size of the disperse phase.

### Molecular orientation of the PET phase

The calculated Hermans orientation factors of the amorphous and crystalline PET phases of the PET/LCP blends are summarized in Table I. The orientation of the PET *trans* conformers was represented by the orientation factors of the bands at 974 and 1340  $\text{cm}^{-1}$ . The orientation of the PET *gauche* conformers was represented by the orientation factors of the bands at 1453 and 1370  $\text{cm}^{-1}$ .

Regarding the composition, it can be observed that the addition of the LCPs to the PET did not have influence on its crystalline orientation, however this addition increased the amorphous phase orientation of the PET in the blends. For better visualization of this result, Figure 8 shows the orientation in the draw direction of the PET phases, amorphous and crystalline, for the PET/LCP Vectra<sup>®</sup> A950 blends.

Concerning the orientation along the transverse section of the extruded films, it can be observed that the orientation of the crystalline and amorphous phase of the PET in the blends slightly increased toward the wall, having a maximum near the wall, where the shear rate is maxima, as mentioned earlier. Both PET/LCP systems showed similar behaviors; however the

PET amorphous phase orientation degree is slightly higher in the PET/LCP Vectra<sup>®</sup> A950 blends. This behavior is shown in Figure 8.

Concerning the behavior of the PET phase molecular orientation in the PET/LCP blends as a function of the LCPs contents, it was observed that the average molecular orientation in the draw direction of the *gauche* segments of the PET chains increased with the increased of both LCPs. The 95/5 PET/LCP blends,

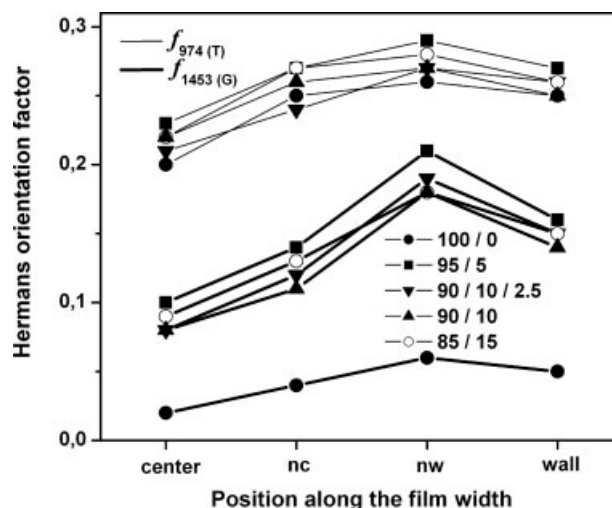


**Figure 8** Hermans orientation factors of the 974- $\text{cm}^{-1}$  and 1453- $\text{cm}^{-1}$  bands along the transverse section of the extruded film of the PET/LCP Vectra<sup>®</sup> A950 blends.

for both LCPs, showed the highest increase followed by the compatibilized and the 90/10 PET/LCP blends. No clear trend was observed in the behavior of both 85/15 PET/LCP blends as a function of LCP content. The reason for the 85/15 blend behavior is not understood. One possible explanation is that for this particular composition, a highly heterogeneous LCP phase morphology<sup>34</sup> was obtained. The influence of the LCP composition on the molecular orientation of the *trans* conformers proved insignificant. The calculated factors for all blends composition had a small variation in the same range as the measurement error. This result will be better discussed in another paper,<sup>33</sup> where the crystal orientation and crystallinity of PET phase were measured by wide angle X-ray diffraction.

The crystallinity degree of the same extruded films was characterized by differential scanning calorimetry.<sup>34</sup> A low percentage of crystallinity, less than 9%, for the pure PET film was obtained; this crystallinity increased only 1.9% when the LCP was added. Therefore, no *gauche-trans* conformational conversion was expected in these films.

The degree of orientation and the *trans* conformer content remained practically constant, while the orientation of the *gauche* conformers markedly increased by the presence of LCP. These observations give evidence of the ordering of the polymer chains in the amorphous phase induced by the presence of LCP. This result does not exclude the possibility of a process involving orientation of *trans* segments in the amorphous phase, as the amorphous phase also contains some *trans* conformers that give rise to a CH<sub>2</sub> wagging band at 1338 cm<sup>-1</sup> and a weak C—O stretching band at 979 cm<sup>-1</sup>.<sup>45</sup>

Figure 9 shows the Hermans orientation factor of the amorphous and crystalline PET phases versus

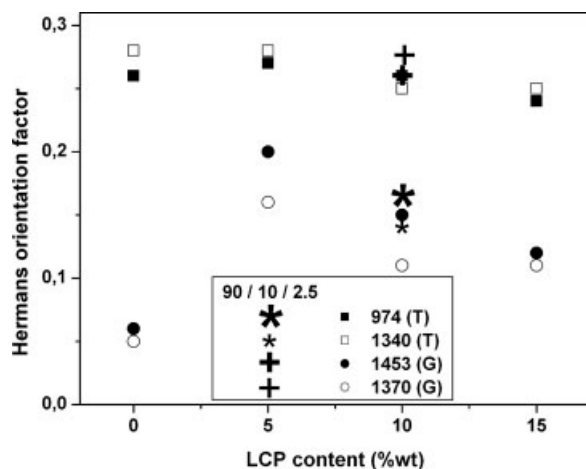


**Figure 9** Hermans orientation factors of the 974-, 1340-, 1370-, and 1453-cm<sup>-1</sup> bands of the PET/LCP Rodrun<sup>®</sup>LC5000 blends as a function of the LCP contents and measured at the position near the films wall.

blend composition for the PET/LCP Rodrun<sup>®</sup>LC5000 system. In this example, the factors were measured at the position near the wall. The orientation factors of the PET phases for the compatibilized PET/LCP blends are also shown. Comparing the compatibilized blend, 90/10/2.5 with the 90/10 PET/LCP blend, it is again clear that the compatibilization was effective mainly for the PET/LCP Vectra<sup>®</sup>A950 blends. The molecular orientation of the amorphous PET phase was increased by the presence of the compatibilizer agent Lotader<sup>®</sup>AX8900. Heino and coworkers<sup>46</sup> showed that the use of this compatibilizer was very effective in the compatibilization of PET with Vectra<sup>®</sup>A950. It was verified that in blends of polyesters like PET and poly(butylene terephthalate) with LCP, the compatibilizer can react with the matrix and with the LCP, since the polyesters are not completely inert.

It can be concluded that there was an alignment of the amorphous PET phase in the draw direction and that this alignment was due to the presence of LCP and of compatibilizer agent.

## CONCLUSIONS

The polarized IR spectroscopy technique was successfully applied to characterize the uniaxial molecular orientation of extruded films of PET/LCP blends. It was observed that due to processing conditions, both LCPs had a relative high degree of uniaxial molecular orientation in the draw direction. However, when blended with PET, the degree of orientation of the LCP phase decreased drastically. An alignment of the amorphous phase of the PET in the draw direction was also verified. In contrast, the PET crystalline phase did not have a substantial orientation in the draw direction. The molecular orientation of the LCP phase and of the PET amorphous phase and the adhesion between the PET and LCP phases were high for the Vectra<sup>®</sup>A950 LCP relative to the Rodrun<sup>®</sup>LC5000 LCP. The orientation of the LCP and the PET amorphous phases varied along the transverse section of the extruded films and as a function of the LCP content, as the orientation maxima at the position where the shear rate was maxima and for the blend with 5 wt% LCP.

The authors are grateful to Rhodia Ster of Brazil for the PET donation.

## References

- Pirnia, A.; Suang, C. S. P. *Macromolecules* 1988, 21, 2699.
- Aji, A.; Brisson, J.; Qu, Y. *J Polym Sci Polym Phys Ed* 1989, 30, 505.
- Kyotani, M.; Kaito, A.; Nakayama, K. *Polymer* 1992, 33, 4756.
- Moon, H. S.; Park, J. K.; Liu, J. H. *J Appl Polym Sci* 1996, 59, 489.
- Chang, J. H.; Jo, B. W. *J Appl Polym Sci* 1996, 60, 939.

6. Moon, H. S.; Park, J. K.; Liu, J. H. *J Appl Polym Sci* 1996, 59, 489.
7. Eijndhoven-Rivera, M. J. V.; Wagner, N. J.; Hsiao, B. *J Polym Sci Part B: Polym Phys* 1998, 36, 1769.
8. Cardoso, G.; Kaito, A.; Bretas, R. E. S. In *Proceedings of the 15th Annual Meeting of the Polymer Processing Society (PPS-15)*; The Netherlands, 1999. p 300.
9. Minkova, L. I.; Velcheva, M.; Paci, M.; Magagnini, P.; La Mantia, F. P.; Sek, D. *J Polym Sci* 1999, 73, 2069.
10. Saengsuwan, S.; Mitchell, G. R.; Bualek-Limcharoen, S. *Polymer* 2003, 44, 5951.
11. Nakinpong, T.; Bualek-Limcharoen, S.; Bhutton, A.; Aungsupravate, O.; Amornsakchai, T. *J Appl Polym Sci* 2002, 84, 561.
12. Bretas, R. E. S.; Baird, D. G. *Polymer* 1992, 24, 5233.
13. Carvalho, B.; Bretas, R. E. S. *J Appl Polym Sci* 1995, 55, 233.
14. Gabellini, G.; Bretas, R. E. S. *J Appl Polym Sci* 1996, 61, 1803.
15. Silva, L. B.; Bretas, R. E. S. *Polym Eng Sci* 2000, 40, 1414.
16. Silva, L. B.; Marinelli, A. L.; Rúvolo, F. A.; Bretas, R. E. S. *Polym Eng Sci* 2002, 42, 1694.
17. Marinelli, A. L.; Bretas, R. E. S. *J Appl Polym Sci* 2003, 87, 916.
18. Ko, C. U.; Wilkes, G. L.; Wong, C. P. *J Appl Polym Sci* 1989, 37, 3063.
19. Mithal, A. K.; Tayebi, A.; Lin, C. H. *Polym Eng Sci* 1991, 31, 1533.
20. Li, J. X.; Silverstein, M. S.; Hitner, A.; Baer, E. *J Appl Polym Sci* 1992, 44, 1531.
21. Heino, M. T.; Seppala, J. W. *J Appl Polym Sci* 1992, 44, 2185.
22. Sukhadia, A. M.; Datta, A.; Baird, D. G. *Int Polym Proc* 1992, 7, 218.
23. Bensaad, S.; Jasse, B.; Noel, C. *Polymer* 1999, 40, 7295.
24. Bensaad, S.; Jasse, B.; Noel, C. *Polymer* 1993, 34, 1602.
25. Kaito, A.; Kyotani, M.; Nikayama, K. *J Polym Sci Part B: Polym Phys* 1993, 31, 1099.
26. Kaito, A.; Nikayama, K.; Kyotani, M. *J Polym Sci Part B: Polym Phys* 1991, 29, 1321.
27. Kaito, A.; Kyotani, M.; Nikayama, K. *Macromolecules* 1991, 24, 3244.
28. Kaito, A.; Kyotani, M.; Nikayama, K. *J Appl Polym Sci* 1995, 55, 1489.
29. Aiji, A.; Cole, K. C.; Dumoulin, M. M.; Ward, I. M. *Polym Eng Sci* 1997, 37, 1801.
30. Cole, K. C.; Daly, H. B.; Sanschagrín, B.; Nguyen, K. T.; Aiji, A. *Polymer* 1999, 40, 3505.
31. Lu, X. F.; Hay, J. N. *Polymer* 2001, 42, 8055.
32. Radhakrishnan, J.; Kaito, A. *Polymer* 2001, 42, 3859.
33. Branciforti, M. C.; Machado, R.; Bretas, R. E. S. (in preparation).
34. Silva, L. B. PhD thesis; Federal University of São Carlos: São Carlos, Brazil, 2003.
35. Wiberg, G.; Gedde, U. W. *Polymer* 1997, 38, 5753.
36. Cole, K. C.; Guèvremont, J.; Aiji, A.; Dumoulin, M. M. *Appl Spectrom* 1994, 48, 1513.
37. Spiby, P.; O'Neill, M. A.; Duckett, R. A.; Ward, I. M. *Polymer* 1992, 33, 4479.
38. Zhang, X.; Aiji, A.; Jean-Marie, V. *Polymer* 2001, 42, 8179.
39. Matthews, R. G.; Aiji, A.; Dumoulin, M. M.; Prud'homme, R. *Polym Eng Sci* 1999, 99, 2377.
40. Guèvremont, J.; Aiji, A.; Cole, K. C.; Dumoulin, M. M. *Polymer* 1995, 36, 3385.
41. Qureshi, N.; Stepanov, E. V.; Schiraldi, D.; Hiltner, A.; Baer, E. *J Polym Sci Part B: Polym Phys* 2000, 38, 1679.
42. Silva, L. B.; Ueki, M. M.; Farah, M.; Barroso, V. M. C.; Maia, J. M. L. P.; Bretas, R. E. S. *Rheol Acta* 2005, 37, 1.
43. Bretas, R. E. S.; D'ávila, M. A. *Reologia de Polímeros Fundidos*, 2nd ed.; EDUFSCar: Sao Carlos, Brazil, 2005.
44. Paul, D. R.; Bucknall, C. B. *Polymer Blends Formulations*, Vol. 1; Wiley: New York, 2000.
45. Hutchinson, I. J.; Ward, I. M.; Willis, H. A.; Zichy, V. *Polymer* 1980, 21, 55.
46. Heino, M.; Seppala, J. E.; Westman, M. U.S. Pat. 525/133 (2001).